

Porous Metal–Organic Frameworks for Heterogeneous Biomimetic Catalysis

Min Zhao, Sha Ou, and Chuan-De Wu*

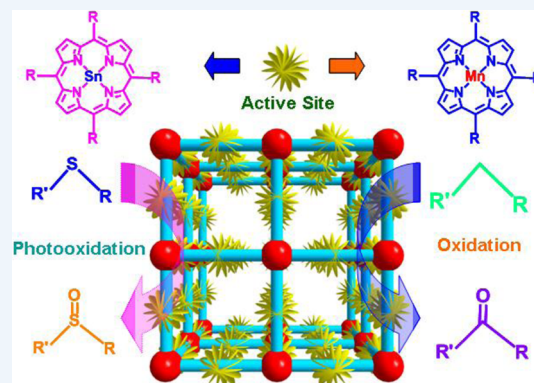
Center for Chemistry of High-Performance and Novel Materials, Department of Chemistry, Zhejiang University, Hangzhou 310027, P. R. China

ABSTRACT: Metalloporphyrins are the active sites in monooxygenases that oxidize a variety of substrates efficiently and under mild conditions. Researchers have developed artificial metalloporphyrins, but these structures have had limited catalytic applications. Homogeneous artificial metalloporphyrins can undergo catalytic deactivation via suicidal self-oxidation, which lowers their catalytic activity and sustainability relative to their counterparts in Nature. Heme molecules in protein scaffolds can maintain high efficiency over numerous catalytic cycles. Therefore, we wondered if immobilizing metalloporphyrin moieties within porous metal–organic frameworks (MOFs) could stabilize these structures and facilitate the molecular recognition of substrates and produce highly efficient biomimetic catalysis.

In this Account, we describe our research to develop multifunctional porphyrinic frameworks as highly efficient heterogeneous biomimetic catalysts. Our studies indicate that porous porphyrinic frameworks provide an excellent platform for mimicking the activity of bio-

catalysts and developing new heterogeneous catalysts that effect new chemical transformations under mild conditions.

The porous structures and framework topologies of the porphyrinic frameworks depend on the configurations, coordination donors, and porphyrin metal ions of the metalloporphyrin moieties. To improve the activity of porous porphyrinic frameworks, we have developed a two-step synthesis that introduces the functional polyoxometalates (POMs) into POM-porphyrin hybrid materials. To tune the pore structures and the catalytic properties of porphyrinic frameworks, we have designed metalloporphyrin $M\text{-H}_8\text{OCPP}$ ligands with four *m*-benzenedicarboxylate moieties, and introduced the secondary auxiliary ligands. The porphyrin metal ions and the secondary functional moieties that are incorporated into porous metal–organic frameworks greatly influence the catalytic properties and activities of porphyrinic frameworks in different reactions, such as the oxidation of alkylbenzenes, olefins, and hexane and the photo-oxygenation of 1,5-dihydroxynaphthalene and sulfides. The porphyrin metal ions and the secondary auxiliary sites in the pores can work together synergistically to enhance the catalytic activities of porphyrinic frameworks. Compared with their homogeneous counterparts, the activities and stabilities of the heterogeneous porphyrinic frameworks are remarkable: the immobilization of metalloporphyrins onto the pore surfaces of MOFs not only prevents their suicidal self-oxidation but also allows them to activate inert substrate molecules, such as cyclohexane. Moreover, because the bulky molecules cannot easily access the active sites inside the pores of porphyrinic frameworks, these porous materials demonstrate interesting size-selective catalytic properties toward substrates.



1. INTRODUCTION

Metal–organic frameworks (MOFs), an emerging new class of porous materials, are self-assembled from organic linkers and inorganic connectors of metal ions and/or clusters.^{1,2} Developed at an extraordinary pace over the past two decades, MOF materials not only enrich the domain of porous materials, but also lead to a number of applications in gas storage and separation, sensing, magnetics, luminescence, catalysis and drug delivery, and so forth.^{3–14}

Because of their unique chemical, physical, and electronic properties and their functions on molecular binding, catalysis, light harvesting, and energy and electron transfers, large amounts of porphyrins and their metal derivatives have been extensively explored to understand and mimic the functionalities of natural biological systems.^{15–18} As organic linkers have played crucial roles in targeting the functionalities of porous MOFs, porphyrins

and metalloporphyrins have received great attention in building porous porphyrinic framework materials for their diverse applications.^{19–23}

Incorporation of porphyrin and metalloporphyrin moieties into the emerging porous MOF materials not only can retain and enhance the functionalities of the building blocks, but also can generate new functionalities. This is because the porphyrin-containing building blocks can be stabilized in the formed solid frameworks, while the pore structures of the framework materials can lead to their differential recognitions of the substrates. Furthermore, the catalytic functionalities of the porous porphyrinic framework materials can be easily realized by modulating

Received: November 5, 2013

Published: February 6, 2014

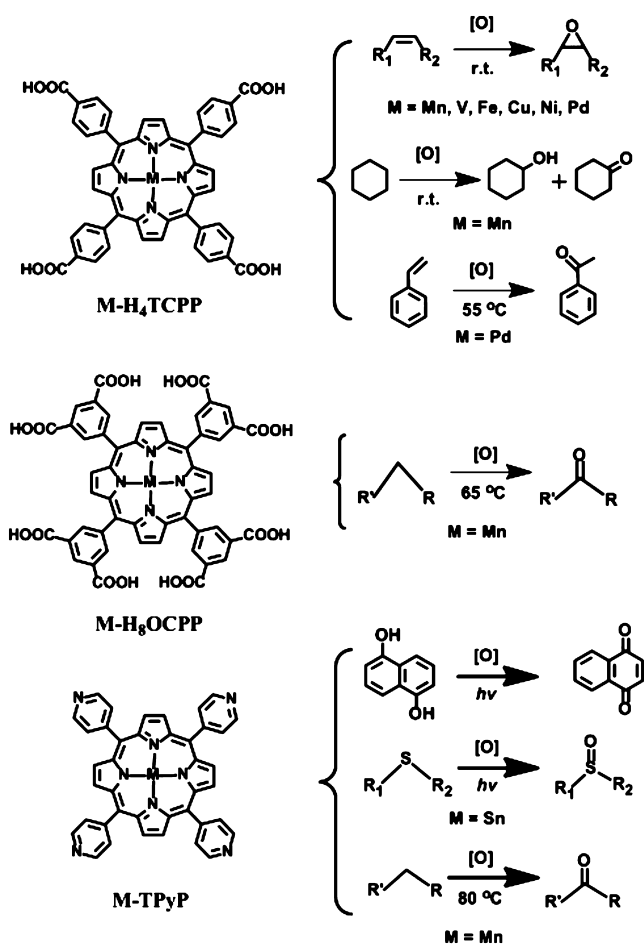
catalytic-active metal sites and tailoring the peripheral environments of metalloporphyrins.

Our group has been working on the synthesis of porous porphyrinic frameworks and exploration of these new MOF materials for their heterogeneous biomimetic catalysis over the past several years. This Account summarizes our progress on the porous porphyrinic frameworks for the selective oxidation of alkenes, alkanes and phenylalkanes, and photo-oxygenation of phenol and sulfides.

2. SYNTHESIS STRATEGY

Although precise prediction of the self-assembled coordination networks remains a challenge, it is feasible to carefully select organic and inorganic components with tailored properties for the construction of porous porphyrinic frameworks. As a class of multidentate ligands, as shown in Scheme 1, porphyrins can

Scheme 1. Metalloporphyrin Ligands Used for the Construction of Porphyrinic Frameworks and Their Catalytic Reactions in this Account^a



^aM-H₄TCPP = metal-tetrakis(4-carboxyphenyl)porphyrin; M-H₈OCPP = metal-5,10,15,20-tetrakis(3,5-bis(carboxylphenyl))porphyrin; M-TPyP = metal-5,10,15,20-tetra(4-pyridyl)porphyrin.

coordinate with different metal ions in multiple coordination modes to direct the formation of different framework structures for their catalytic applications. Among the reported methods, solvothermal reaction is frequently used to control the structures of porphyrinic frameworks by modulating the reaction media, thermal ramping, and temperature, etc.

The structures of porphyrinic frameworks are dependent on the reaction conditions, metal nodes, and porphyrin peripheries, and can be further tuned by the porphyrin metal ions, as demonstrated in the five MOFs [Pb₂(H₂TCPP)]·guest (1; guest = lattice solvent molecules), Pb₂(Co-TCPP)(H₂O)(DMF)]·guest (2), [Pb₂(Ni-TCPP)(DMF)(H₂O)]·guest (3), [Pb₂(Cu-TCPP)(DMF)(H₂O)]·guest (4), and [Pb₂(VO-TCPP)(H₂O)₂]·guest (5).²⁴ Due to the large ionic radius, variable coordination number and flexible coordination sphere of the heavy p-block lead(II) ion, the constituent organic and inorganic components within these MOFs are tightly compacted because “Nature Abhors the Vacuum”. In their structures, the different coordination geometries of porphyrin metals, such as the four-coordinated Co^{II}, Ni^{II} and Cu^{II} squares, five-coordinated V^{IV} square-pyramid, let TCPP scaffolds differ in the conformations of porphyrin macrocycles (Figure 1). The different M-TCPP ligands further

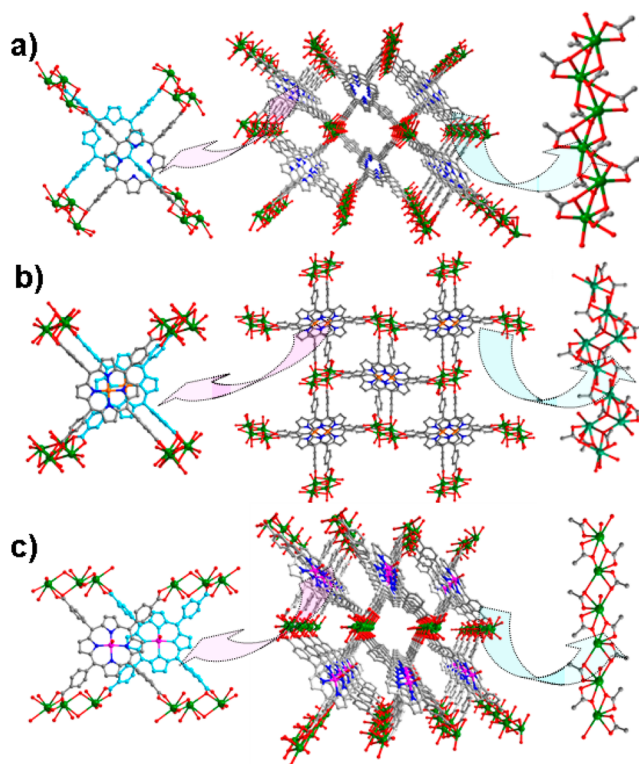


Figure 1. Structures of (a) [Pb₂(H₂TCPP)], (b) [Pb₂(M-TCPP)(DMF)(H₂O)] (M = Co^{II}, Ni^{II}, and Cu^{II}), and (c) [Pb₂(VO-TCPP)(H₂O)₂]. Left: views of the arrangements of the porphyrin macrocycles. Middle: views of the 3D representative porous frameworks. Right: side views of the 1D polymeric chains of carboxyl oxygen bridging Pb²⁺ ions. Color scheme: Pb, green; O, red; N, blue; C, gray; M, orange; V, pink. Reproduced with permission from ref 24. Copyright 2012 Royal Society of Chemistry.

manipulate the stacking of the TCPP moieties and the coordination spheres of Pb²⁺ ions. As a consequence, Pb²⁺ ions are triply (M = H₂), triply and doubly (M = Co^{II}, Ni^{II}, and Cu^{II}) or doubly (M = V^{IV}O) bridged by the carboxyl oxygen atoms in the polymeric chains of the different porphyrinic frameworks. On the other hand, the coordination driving force between TCPP and Pb²⁺ nodes inversely affects the configurations of porphyrin rings for the generation of different porphyrin core dependent networks.

If the porphyrin macrocycles cannot be closely packed, the porphyrinic frameworks are only slightly responsive to the

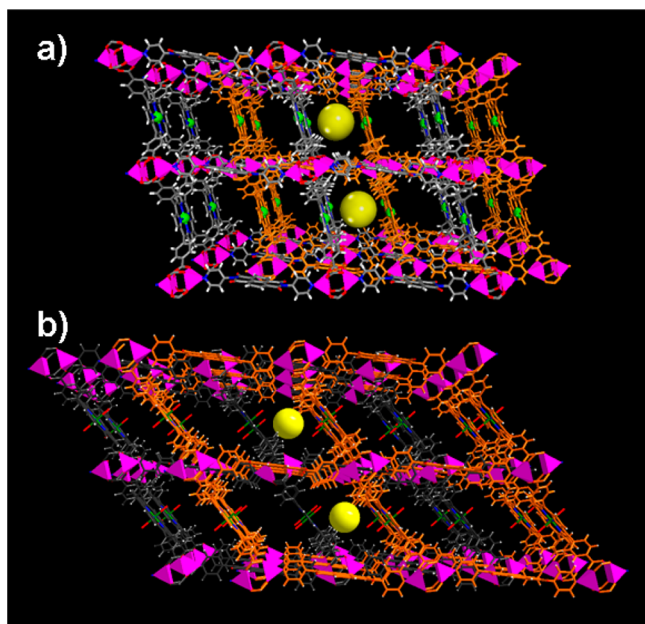


Figure 2. Crystal structures of the twofold interpenetrated 3D nets of (a) CZJ-1-Cu and (b) CZJ-1-Mn viewed along the channels, in which the metal sites have been uniformly immobilized on the pore surfaces. The large yellow balls are used to highlight the different pore sizes. Color scheme: Cu, green; Mn, dark green; Zn, pink-square pyramids; O, red; N, blue; C, gray; H, light gray. Reprinted with permission from ref 25. Copyright 2013 Wiley-VCH.

porphyrin metal sites. As shown in Figure 2, the porphyrin metal effect is not obvious in the six porphyrinic frameworks $[\text{Zn}_2(\text{MX-TCPP})(\text{DPNI})] \cdot (\text{guest})_x$ (CZJ-1-Mn, MX = $\text{Mn}^{\text{III}}\text{OH}$; CZJ-1-Cu, MX = Cu^{II} ; CZJ-1-Ni, MX = Ni^{II} ; CZJ-1-Pd, MX = Pd^{II} ; CZJ-1-Fe, MX = $\text{Fe}^{\text{III}}\text{Cl}$ and CZJ-1-V, MX = $\text{V}^{\text{IV}}\text{O}$; DPNI = N,N'-di-(4-pyridyl)-1,4,5,8-naphthalenetetracarboxydiimide), which have the same doubly interpenetrated cubic α -Po topology.²⁵ In the crystal structures, the basic $\text{Zn}_2(\text{COO})_4$ paddle-wheel clusters as the secondary building units (SBUs) are bridged by MX-TCPP to form 2D sheets which are further connected by the organic linker DPNI to form their 3D porous structures. Their crystal packing and thus the pore structures are slightly different depending on the axial porphyrin metal sites. They can be classified into two types: (a) CZJ-1-Cu, CZJ-1-Ni, and CZJ-1-Pd that do not have axial coordination site with the free pore spaces of $\sim 60\%$; and (b) CZJ-1-Mn, CZJ-1-Fe and CZJ-1-V that have axial coordination sites with the accessible pore volumes of $\sim 52\%$. Such different accessible pore volumes have also been reflected on their slightly different pore channels. As shown in Figure 2 for their representative pore structures, CZJ-1-Cu has the larger pores of $7.8 \times 8.5 \text{ \AA}^2$, while CZJ-1-Mn has the smaller pores of about $6.1 \times 7.8 \text{ \AA}^2$. Such a strategy by making use of two types of linkers to rationally immobilize different metal sites into the pore surfaces of the isomorphous porphyrinic frameworks is very important to simply target their different catalytic functions.

Polyoxometalates (POMs) are a unique class of anionic metal–oxygen clusters, which have been the functional constituents in a variety of solid materials.²⁶ Combination of POMs and metalloporphyrins into porous hybrid materials will not only retain the individual functionalities but also exhibit new and unique features. However, these two moieties have the adverse solubility in either hydrophilic (POMs) or hydrophobic (porphyrins) solvents which makes the synthesis of metalloporphyrin-POM-based

hybrids extremely difficult. To resolve their distinct solubility issue under moderate reaction conditions, an efficient strategy was therefore developed by reaction of POMs with porphyrins to form zwitterionic complexes at the first step. The combined components are soluble both in water and common organic solvents. By this strategy, $\{[\text{Cd}(\text{DMF})_2\text{Mn}^{\text{III}}(\text{DMF})_2\text{TPyP}](\text{PW}_{12}\text{O}_{40})\} \cdot \text{guest}$ (**6**) was synthesized upon reaction of a mixture of the zwitterionic complex with cadmium nitrate under mild conditions, which paves a new pathway for the synthesis of POM-porphyrin hybrid materials.²⁷ The structure of **6**, containing large cavities of $10.07 \times 10.09 \times 12.44 \text{ \AA}^3$ and 1D opening channels of $5.36 \times 12.44 \text{ \AA}^2$, is built on alternate layers of POM anions and cationic metal-porphyrin nets (Figure 3). The hybrid solid **6** demonstrates remarkable stability under different conditions and high capture capability for scavenging different dyes from their water solutions.

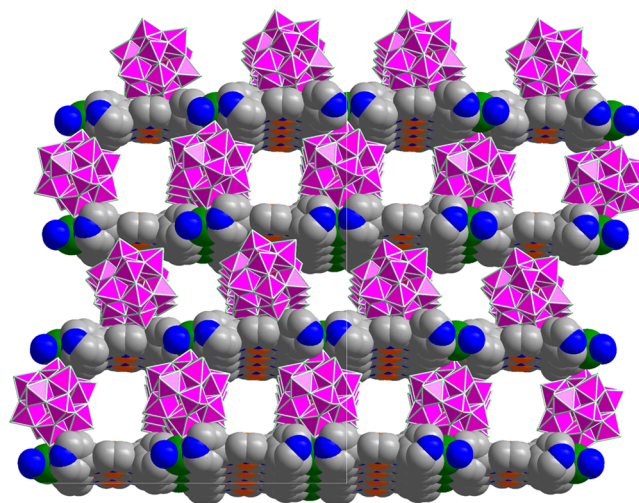


Figure 3. Space-filling and polyhedral representations of the porous structure of **6**, building from two kinds of alternate layers of POM anions and cationic Mn^{III} -porphyrin nets. Color scheme: Mn, orange; Cd, green; W, pink octahedra; N, blue; C, gray.

3. CATALYTIC APPLICATION OF PORPHYRINIC FRAMEWORKS

As an emerging class of porous materials that consist of metalloporphyrin units, porphyrinic frameworks definitely comprehend the properties in their original application fields. The applications include gas storage and separation,^{28,29} selective sorption of guest molecules,³⁰ nanofilms,³¹ and light harvesting.³² Moreover, incorporation of the heme analogues of metalloporphyrins into porous MOFs renders porphyrinic frameworks highly active and stable in heterogeneous biomimetic catalysis with interesting size- and/or shape-selective properties.^{19,33–37}

3.1. Fe-Porphyrins as Lewis Acid Sites for Aldol Reaction

Fe-porphyrins are expected as ideal synthons for crystal engineering of porous MOFs as a unique platform for biomimetic catalysis with heme analogues in control over porous ambient. The 3D structure of $[\text{Zn}_2(\text{HCOO})(\text{Fe}^{\text{III}}(\text{H}_2\text{O})\text{-TCPP})] \cdot \text{guest}$ (**7**) is made up of layered network of Fe^{III} -TCPP connected with binuclear $\text{Zn}_2(\text{COO})_4$ paddle-wheel SBUs, and further linked by formate pillars to homogeneously coordinate with $\text{Zn}_2(\text{COO})_4$ SBUs (Figure 4a).³⁸ As shown in Figure 4b, when Cd^{2+} ions were used as connecting nodes, two Fe^{III} -HTCPP ligands are coupled by one μ_2 -oxo to form a dimer, which performs as a decadentate

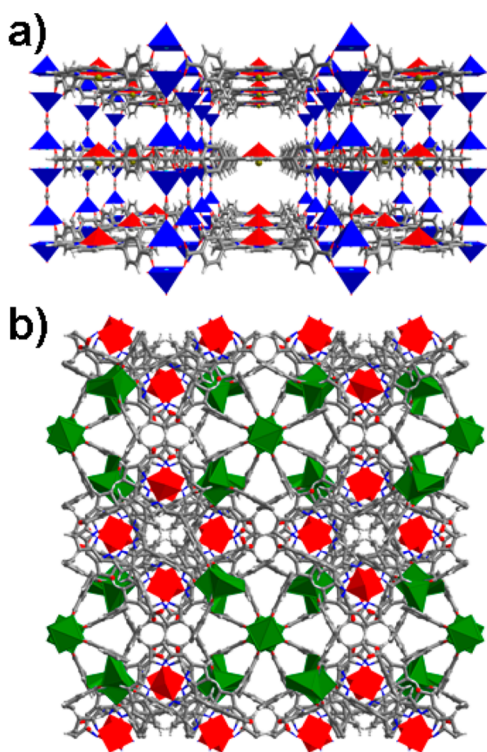


Figure 4. (a) Perspective view of the 3D porous structure of **7**, showing the opening channels and the uniformly dispersed Fe^{III} centers on the pore surfaces. (b) View of the 3D microporous structure of **8** along the screw 4_1 axis. Color scheme: Fe, red square-pyramids; Zn, blue square-pyramids; O, red; N, blue; C, gray; H, light gray; Cd, green polyhedra. Reproduced with permission from ref 38. Copyright 2013 American Chemical Society.

ligand to bridge ten Cd^{II} ions into a 3D microporous framework of $[\text{Cd}_3(\text{H}_2\text{O})_6(\mu_2\text{-O})(\text{Fe}^{\text{III}}\text{-HTCPP})_2]\cdot\text{guest}$ (**8**). In their crystal structures, the square-pyramidally coordinated iron(III) ions are out of the porphyrin plane, which orient toward the pores that are accessible to the included solvent molecules. However, they are not efficient on styrene catalytic oxidation with iodosobenzene (PhIO) oxidant at room temperature (17.9 and 8.4% yields of epoxidized product for **7** and **8**, respectively). The less oxidation efficiency is a consequence of the self-oxidation of the individual pyrrolic rings that are evident from bleaching out the reaction mixture. It is interesting that the porphyrinic frameworks **7** and **8** are highly active on the intermolecular aldol reaction of aldehydes and ketones under solvent free conditions, in which up to 99% yield of aldol product was achieved (Scheme 2). The catalytic efficiency is superior to their homogeneous counterparts, such as FeCl–Me₄TCPP, Zn(NO₃)₂, Cd(NO₃)₂ and FeCl₃, under otherwise identical conditions.

3.2. Mn-Porphyrins on Solid Surfaces as Active Sites for Oxidation Reaction

Mn-porphyrins, the heme cofactor analogues of cytochrome P450 enzymes, can efficiently oxidize a variety of organic molecules. However, the axial sites of the octahedrally coordinated Mn^{III} ions are easily ligated by additional ligands in porphyrinic frameworks, which obstruct their catalytic application. As shown in Figure 5, the active Mn^{III} sites in two isomorphous porphyrinic frameworks $[(\text{CH}_3)_3\text{NH}_2][\text{Zn}_2(\text{HCOO})_2(\text{Mn}^{\text{III}}\text{-TCPP})]\cdot\text{guest}$ (**9**) and $[(\text{CH}_3)_2\text{NH}_2][\text{Cd}_2(\text{HCOO})_2(\text{Mn}^{\text{III}}\text{-TCPP})]\cdot\text{guest}$ (**10**) are blocked by formate ligands, which make the active sites inaccessible to substrate molecules through the opening

Scheme 2. Aldol Reaction of Aldehydes with Ketones Catalyzed by **7** and **8** under Solvent Free Conditions

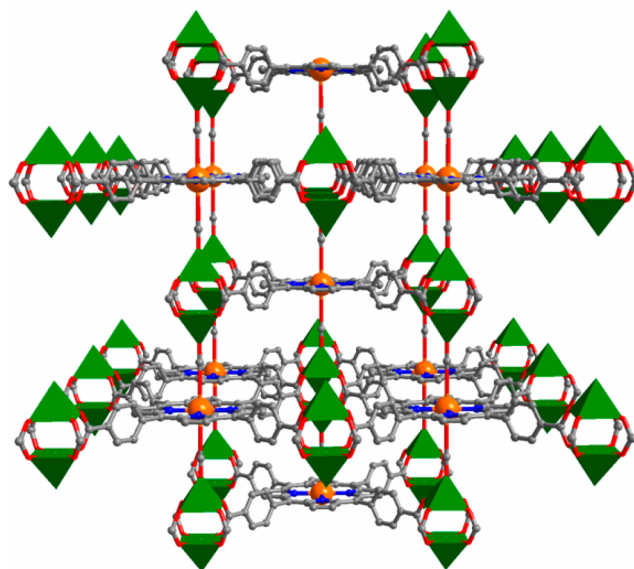
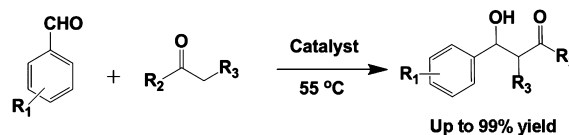
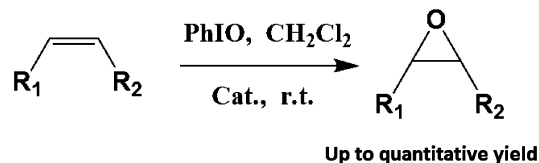


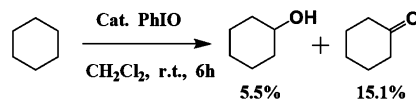
Figure 5. Perspective view of the 3D porous porphyrinic framework of **9**, in which the axial coordination sites of Mn^{III} ions inside the pores have been blocked by formate pillars. Color scheme: Mn, orange balls; Zn, green square-pyramids; O, red; N, blue; C, gray.

channels.³⁸ Hence, the catalysis only occurs on the exterior solid surfaces with coordinative defects of porphyrin Mn^{III} ions on the epoxidation of alkenes (Scheme 3) and oxidation of cyclohexane (Scheme 4). The solid surface promoted catalysis was further demonstrated from the significant particle-size-effect on the oxidation rates.

Scheme 3. Selective Oxidation of Olefins Catalyzed by Solid **9**



Scheme 4. Oxidation of Cyclohexane Catalyzed by Solid **9**



3.3. Pd-Porphyrins as Active Sites for Selective Oxidation of Styrene

The porous coordination network $[\text{Cd}_{1.25}(\text{Pd}\text{-H}_{1.5}\text{TCPP})(\text{H}_2\text{O})]\cdot\text{guest}$ (**11**) comprises square-coordinated palladium(II) sites in the channel walls along with the tailored zeolitic periphery (Figure 6).³⁹ It is interesting that the square-coordinated Pd^{II} ions in TCPP are highly active on oxidation reactions by forming high valent Pd intermediates, as demonstrated in the selective

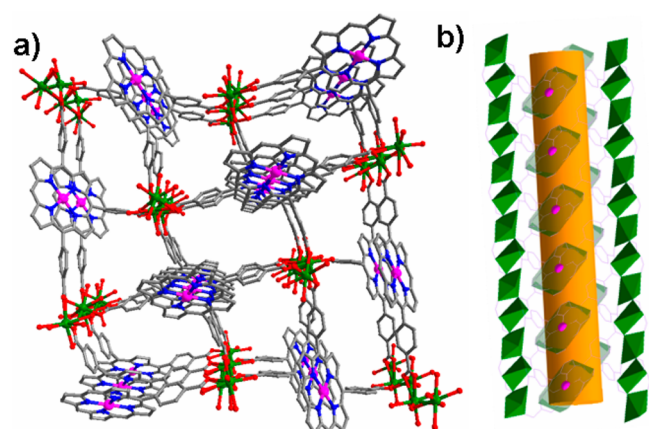


Figure 6. (a) Perspective view of the 3D porous structure of **11** down the *a* axis, and (b) side view of the 1D opening channel and the substrate accessible Pd^{II} sites in **11**. Color scheme: Pd, pink; Cd, green balls and polyhedra; O, red; N, blue; C, gray. Reprinted with permission from ref 39. Copyright 2011 Royal Society of Chemistry.

oxidation of styrene. The styrene was fully oxidized into a mixture of 91% acetophenone and 9% benzaldehyde by **11** with H₂O₂ oxidant at 55 °C in acidified CH₃CN solution. The catalytic property of **11** is superior to its components of Pd–H₄TCPP, PdCl₂, Pd(OAc)₂, and Pd/C on the substrate conversions and product selectivities. The single crystal structure and ¹H NMR spectroscopy clearly indicate that the styrene molecules are readily incorporated into the pores of **11**, which thus demonstrate that the catalytic reaction mainly occurs inside the pores.

3.4. Sn-Porphyrins as Active Sites for Photooxidation Irradiated with Visible Light

Metalloporphyrins are excellent sensitizers for light activation in photosynthesis. However, the homogeneous metalloporphyrins are easily deactivated by photoreaction with the singlet oxygens.⁴⁰ Even though immobilization of the metalloporphyrins on solid matrices can improve their stability; however, it will be inevitable to depress their high photoactivity. As illustrated in the example of [Zn₂(H₂O)₄Sn^{IV}(TPyP)(HCOO)₂] \cdot guest (**12**), such a dilemmatic issue was simply solved by isolation and immobilization of metalloporphyrins in the channel walls of porous MOFs.⁴¹ As shown in Figure 7, the 3D porous structure of **12** is built from lamellar networks of tin(IV)-porphyrin struts linking up Zn nodes which are further connected by formates to

coordinate with Sn^{IV} centers. Solid **12** exhibits remarkable photocatalytic activity on photo-oxygenation of 1,5-dihydroxynaphthalene and sulfides under visible light irradiation. Almost quantitative conversions and remarkable selectivities (up to >99%) are achieved in heterogeneous phases with outstanding stability for the subsequent recycling catalysis.

3.5. Mn-Porphyrins as Main Active Sites with Synergistic Effect for Highly Efficient Oxidation

To incorporate additional functional sites/groups into the emerging porphyrinic frameworks, the 3D periodical arrangements of these moieties within the porous frameworks have enabled them to collaboratively enhance their catalytic activity. Further more, the pore structures will direct their selective molecular recognition, and thus further improve their catalytic selectivity in heterogeneous phases. The M–H₈OCPP ligand having four *m*-benzenedicarboxylate moieties is powerful for the construction of highly porous MOFs, as illustrated in three isostructural porous porphyrinic frameworks, [Mn₃Cl₂(MnCl-OCPP)(DMF)₄(H₂O)₄] \cdot guest (ZJU-18), [Mn₃Cl₂(Ni-OCPP)(H₂O)₈] \cdot guest (ZJU-19), and [Cd₃Cl₂(MnCl-OCPP)(H₂O)₆] \cdot guest (ZJU-20).⁴² As shown in Figure 8, the metalloporphyrin octacarboxylates are bridged by binuclear and trinuclear metal-carboxylate SBUs to form 3-periodic, binodal, edge-transitive net with RCSR symbol *tbo* and pore windows of about 11.5 Å and pore cages of about 21.3 Å in diameters.

ZJU-18 exhibits high efficiency on the oxidation of alkylbenzene with tertbutylhydroperoxide (TBHP) oxidant at 65 °C, in which 99% yield and 8076 turnovers were realized for the transformation of ethylbenzene to acetophenone. The catalytic activity is much higher than that of ZJU-19 (9% conversion) with active metal nodes only, and that of ZJU-20 (69% conversion) with active metalloporphyrin only. The significant differences for their catalytic activities clearly reveal the roles of the Mn^{III}Cl-OCPP sites, the manganese(II) sites on the nodes and their collaborative effect. ZJU-18 is much superior to the homogeneous molecular counterpart Mn^{III}Cl–Me₈OCPP in terms of catalytic activities (>99% for ZJU-18 versus 16% for Mn^{III}Cl–Me₈OCPP) and stabilities (sustained for 15 cycles versus deactivated at the third cycle), indicating that such a porous metalloporphyrinic framework approach has not only heterogenized the homogeneous catalysts, but also significantly enhanced their catalytic activities by synergizing multiple effects. Because the catalysis mainly occurs inside the pores, ZJU-18 exhibits size-selectivity in the oxidation of different alkylbenzenes.

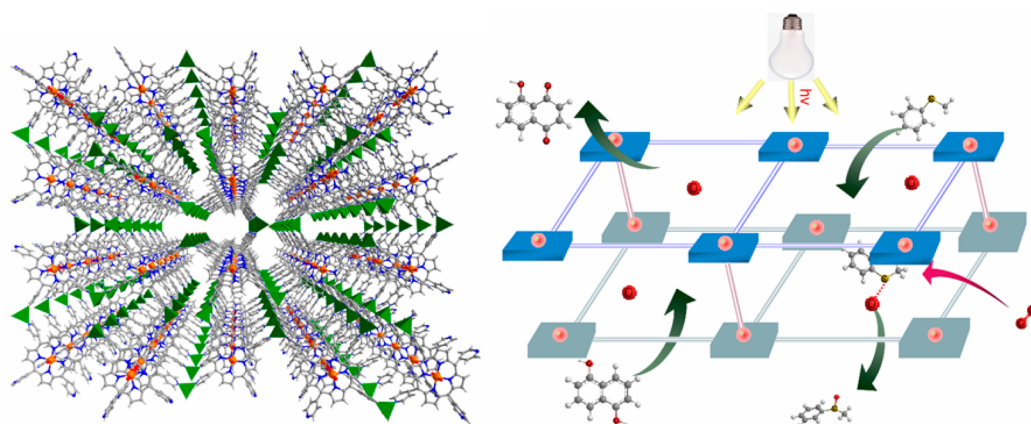


Figure 7. Perspective view of the 3D porous framework of **12** down the *c* axis (left) and schematic representation of the photooxidation of phenol and sulfides (right). Color scheme: Sn, orange balls; Zn, green square-pyramids; O, red; N, blue; C, gray; H, light gray.

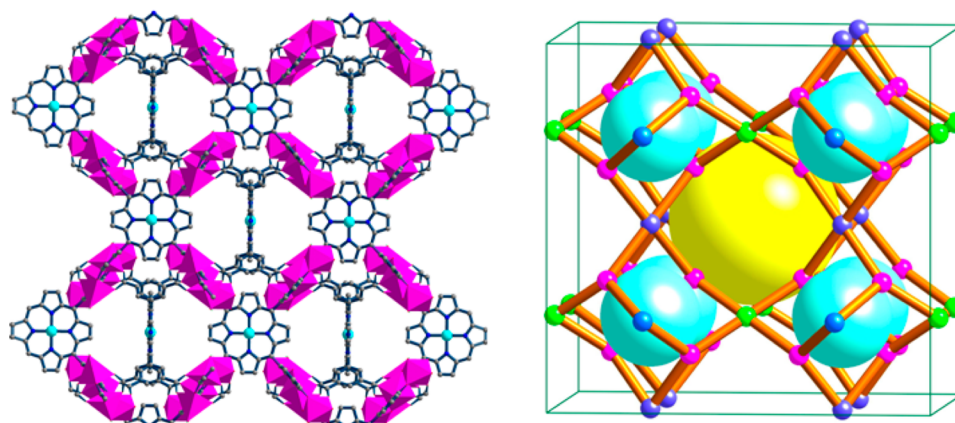
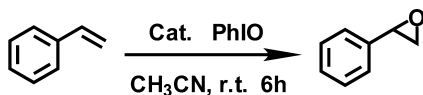


Figure 8. The 3D porous crystal structure (left) and the *tbo* topology (right) of ZJU-18, showing the substrate accessible catalytically active Mn sites inside the pores (large yellow and cyan balls represent the large and small cavities, respectively). Color scheme: Mn, small cyan balls and pink octahedra; N, blue; C, gray. Reproduced with permission from ref 42. Copyright 2012 American Chemical Society.

Another advantage of the metalloporphyrinic framework approach is to systematically immobilize different metal sites into porphyrins to tune the catalytic properties. As demonstrated in CZJ-1-Mn, CZJ-1-Cu, CZJ-1-Ni, CZJ-1-Pd, CZJ-1-Fe, and CZJ-1-V, different metal sites as well as additional organic ligands can be readily immobilized into their pores.²⁵ These porphyrinic frameworks have distinct catalytic properties on the epoxidation of styrene at room temperature. As shown in Table 1, CZJ-1-M

Table 1. Selective Epoxidation of Styrene Catalyzed by CZJ-1-M^a



entry	catalyst	conv (%) ^b	select (%) ^b
1	CZJ-1-Fe	34	97
2	CZJ-1-Pd	<1	47
3	CZJ-1-V	<1	47
4	CZJ-1-Ni	<1	46
5	CZJ-1-Cu	<1	
6	CZJ-1-Mn	>99	98

^aStyrene (0.1 mmol), PhIO (0.15 mmol), catalyst (0.005 mmol), and CH₃CN (1.5 mL) sealed in a Teflon lined screw cap vial were stirred at room temperature for 6 h. ^bConversion % and selectivity % were determined by GC-MS on a SE-54 column.

(M = Fe^{III}Cl, Pd^{II}, V^{IV}O, Ni^{II} or Cu^{II}) has basically no or very low catalytic activity for the epoxidation of styrene (entries 1–5); however, CZJ-1-Mn exhibits very high catalytic activity in which styrene can be almost fully oxidized into the epoxide product (entry 6). Moreover, catalyst CZJ-1-Mn can be utilized in much less amount but still highly active to achieve 14 068 turnovers. The superior catalytic activity of CZJ-1-Mn was further demonstrated on the oxidation of the most inert cyclohexane with extremely high catalytic activity at room temperature (Scheme 5).

As shown in Figure 9, the fundamental basis for the reaction to take place inside the pores is confirmed by the single crystal structure of CZJ-1-Mn⊃styrene, while the access of the inside active sites was proved by combination of the Ti species with the hydroxyl group on porphyrin Mn^{III} ions in CZJ-1-Mn-Ti. The remarkable catalytic activity of CZJ-1-Mn should be the collaborative work effects of the neighboring Mn^{III}-porphyrins,

Scheme 5. Highly Efficient and Selective Oxidation of Cyclohexane Catalyzed by CZJ-1-Mn

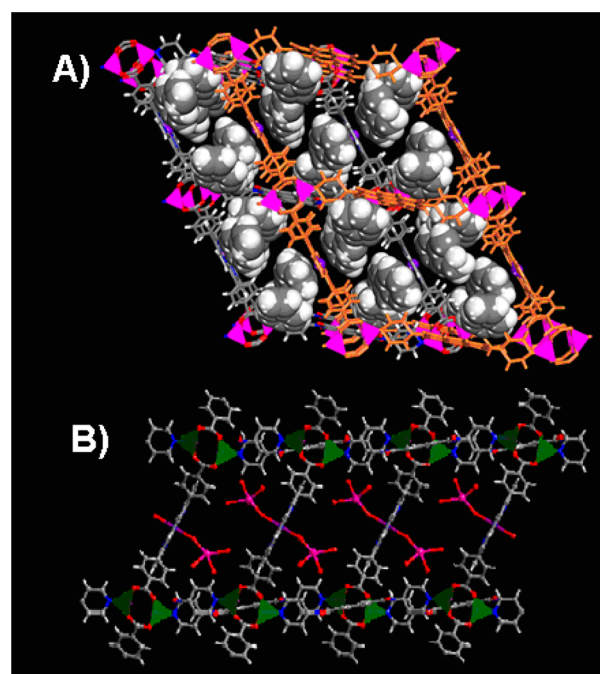
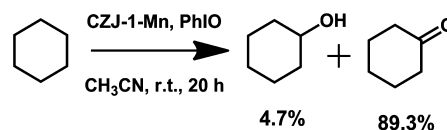


Figure 9. Crystal structures of (a) CZJ-1-Mn⊃styrene (styrene molecules in space-filling model) and (b) CZJ-1-Mn-Ti as viewed along the channels, indicating that the active Mn^{III} sites inside the pores are accessible to substrate molecules. Color scheme: Zn, pink and green square-pyramids; Ti, pink balls; O, red; N, blue; C, gray; H, light gray. Reprinted with permission from ref 25. Copyright 2013 Wiley-VCH.

the flexible structure and the specific electronic environments around the catalytic Mn^{III} sites, tuned by both porphyrin and DPNI moieties. Since the catalysis mainly occurs inside the pores, the bulky 1,1,2,2-tetraphenylethane (~8.2 × 12.7 Å²) cannot be oxidized because it does not have access to the active sites inside the pores.

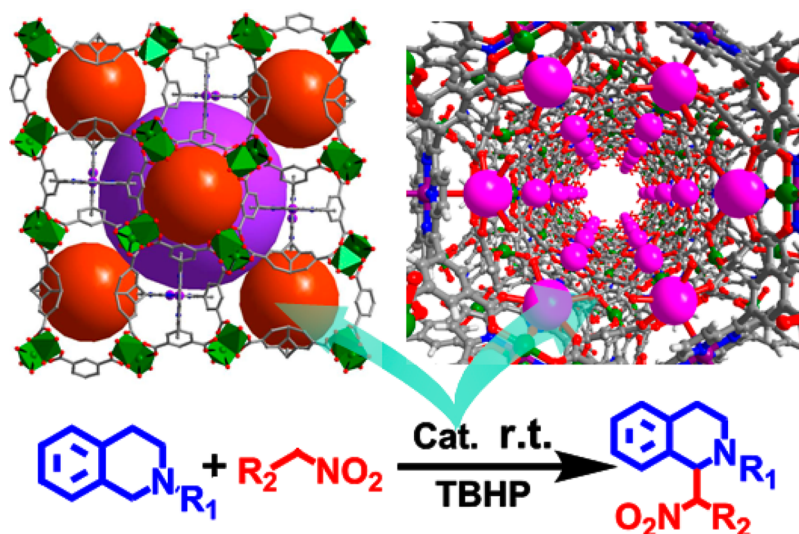


Figure 10. Left: Crystal structure of the 3D *tho* net of ZJU-21. (The large purple and orange balls represent the large and small cages, respectively. Color scheme: Cu, green square-pyramids; Ni, small purple balls; O, red; N, blue; C, gray.) Right: Crystal structure of the 3D *xly* net of ZJU-22, showing the 1D opening nanotubular channels and substrate accessible Cu^{II} sites. (Color scheme: Cu, smaller green and larger pink balls; Mn, violet; O, red; N, blue; C, gray; H, light gray.) Bottom: Catalytic CDC reaction of 1,2,3,4-tetrahydroisoquinoline derivatives with nitroalkanes. Reprinted with permission from ref 43. Copyright 2014 Wiley-VCH.

The introduction of POMs into hybrid materials will improve the interaction between organic substrates and the surfaces of metal oxides to facilitate heterogeneous catalysis. The hybrid material **6**, consisting of the catalytically active Mn^{III}-TPyP species and the interlayered POMs, was able to efficiently oxidize alkylbenzene in H₂O at 80 °C.²⁷ Hybrid **6** oxidizes ethylbenzene to form one product of acetophenone (92.7% yield), which is superior to those of its precursors, such as Mn^{III}Cl-TPyP (73.6% yield of acetophenone) and [PW₁₂O₄₀]³⁻ (inactive). Hybrid **6** also has superior stability over the homogeneous counterpart Mn^{III}Cl-TPyP, because the Mn^{III}-porphyrin sites in the robust layers are separated by [PW₁₂O₄₀]³⁻ polyanions to prevent formation of the inactivated μ-oxo metalloporphyrin dimers.

3.6. Mn-Porphyrins as Pivot Connectors to Stabilize Porous Porphyrinic Framework for Highly Efficient Catalysis

To facilitate heterogeneous catalysis, it requires that the MOF materials have permanent porosity and high stability. However, most of the porphyrinic frameworks are easily decomposed under harsh conditions, which will limit their catalytic application. The two robust porphyrinic frameworks, [Cu₄(Ni^{II}-OCPP)(H₂O)₄]-guest (ZJU-21) and [Cu₁₆(Mn^{III}OCPP)₃(OH)₁₁(H₂O)₁₇]-guest (ZJU-22), are the two exceptional examples which are very stable under various conditions, even in acidified aqueous solution.⁴³ As shown in Figure 10, ZJU-21 is built from Cu₂(COO)₄(H₂O)₂ paddlewheel SBUs and octatopic metal-ligand Ni^{II}-OCPP, forming a 3-periodic, binodal, edge-transitive net that contains nanopore cages (2.1 nm in diameter). The structure of ZJU-22, containing 1D nanotubular channels of 1.5 nm in diameter, can be viewed as a unique 3D framework constructed from three independent nets which are interconnected and stabilized by the Mn–OH–Cu bridges. Although the coordination sites of Mn^{III} ions in ZJU-22 have been fully occupied, however, highly active Cu^{II} sites are immobilized on the pore surfaces of the very stable framework.

The permanent porosities and the accessible Cu²⁺ ions in ZJU-21 and ZJU-22 let them highly active in the Cu-catalyzed cross-dehydrogenative coupling (CDC) reaction of tertiary amines and nitroalkanes under solvent free conditions at room temperature.

Moreover, the accessible Cu^{II} sites within Cu(COO)₂(substrate)_{2–3} in ZJU-22 (up to 97% yield) are more active than the ones within the paddle-wheel Cu₂(COO)₄(substrate)₂ in ZJU-21 (90% yield), because the Cu^{II} sites in ZJU-22 are more easily accessed by substrate molecules inside the pores. The superiority is even more significant when the reactions were carried out in the aqueous solution (93% yield for ZJU-22 vs 66% yield for ZJU-21). Moreover, ZJU-21 and ZJU-22 can promote large scale of tertiary amine substrate (0.420 g) transformation with 80% and 85% isolated yields for ZJU-21 and ZJU-22, respectively.

4. CONCLUSIONS AND FUTURE OUTLOOK

Metalloporphyrins are ideal synthons for the construction of porous crystalline coordination networks. We have outlined several strategies to construct porous porphyrinic frameworks whose structures can be controlled by the coordination driving force between the porphyrin struts and metal nodes. Incorporation of the biomimetic metalloporphyrins into porous metal–organic frameworks, the emerging porous materials not only can sustain their long survival to prevent suicidal self-oxidation but can also enhance catalytic functions. The ability to rationally and systematically tune the pore structures and the catalytically active metal sites has featured the porous porphyrinic frameworks as highly active heterogeneous biomimetic catalysts which exhibit high stabilities, and interesting shape- and size-selectivity on various reactions and thus are superior to their homogeneous molecular counterparts. The research on porous biomimetic MOF catalysts is still in its infancy. It is expected that more extensive research will be carried out on the porous heterogeneous biomimetic MOF catalysts, and some potentially useful catalysts will be realized in the future.

■ AUTHOR INFORMATION

Corresponding Author

*E-mail: cdwu@zju.edu.cn.

Notes

The authors declare no competing financial interest.

Biographies

Min Zhao received her B.S. degree in Chemistry from Yunnan University in 2012. Currently, she is a doctoral student in chemistry at Zhejiang University under the direction of Professor Chuan-De Wu. Her research is focused on the development of porous porphyrinic framework materials for heterogeneous catalysis.

Sha Ou received her B.S. degree in Chemistry from Guizhou University in 2011. Currently, she is a doctoral student in chemistry in Zhejiang University under the direction of Professor Chuan-De Wu. Her research is focused on the development of porous N-heterocyclic carbene-based MOFs for heterogeneous catalysis.

Chuan-De Wu obtained his Ph.D. degree in Physical Chemistry from Fujian Institute of Research on the Structure of Matter, Chinese Academy of Sciences in 2003. He worked as a postdoctoral fellow at the University of North Carolina at Chapel Hill during 2003–2005 before joining Zhejiang University in 2005 as a full professor of chemistry. His research interest focuses on the development of porous framework materials and their heterogeneously catalytic application.

ACKNOWLEDGMENTS

We thank the NSF of China (Grant Nos. 21073158 and 21373180), Zhejiang Provincial Natural Science Foundation of China (Grant No. Z4100038) and the Fundamental Research Funds for the Central Universities (Grant No. 2013FZA3006) for financial support.

REFERENCES

- (1) Long, J. R.; Yaghi, O. M. *Chem. Soc. Rev.* **2009**, *38*, 1213–1504 Themed issues on metal-organic frameworks.
- (2) Zhou, H.-C.; Long, J. R.; Yaghi, O. M. *Chem. Rev.* **2012**, *112*, 673–1268 Metal-Organic Frameworks special issue.
- (3) Li, J.-R.; Kuppler, R. J.; Zhou, H.-C. Selective gas adsorption and separation in metal-organic frameworks. *Chem. Soc. Rev.* **2009**, *38*, 1477–1504.
- (4) Wu, H.; Gong, Q.; Olson, D. H.; Li, J. Commensurate Adsorption of Hydrocarbons and Alcohols in Microporous Metal-Organic Frameworks. *Chem. Rev.* **2012**, *112*, 836–868.
- (5) Kreno, L. E.; Leong, K.; Farha, O. K.; Allendorf, M.; Van Duyne, R. P.; Hupp, J. T. Metal-Organic Framework Materials as Chemical Sensors. *Chem. Rev.* **2011**, *112*, 1105–1125.
- (6) Coronado, E.; Minguez Espallargas, G. Dynamic magnetic MOFs. *Chem. Soc. Rev.* **2013**, *42*, 1525–1539.
- (7) Allendorf, M. D.; Bauer, C. A.; Bhakta, R. K.; Houk, R. J. T. Luminescent metal-organic frameworks. *Chem. Soc. Rev.* **2009**, *38*, 1330–1352.
- (8) Cui, Y.; Yue, Y.; Qian, G.; Chen, B. Luminescent Functional Metal-Organic Frameworks. *Chem. Rev.* **2012**, *112*, 1126–1162.
- (9) Ma, L.; Falkowski, J. M.; Abney, C.; Lin, W. A Series of Isorecticular Chiral Metal-Organic Frameworks as a Tunable Platform for Asymmetric Catalysis. *Nat. Chem.* **2010**, *2*, 838–846.
- (10) Yoon, M.; Srirambalaji, R.; Kim, K. Homochiral Metal-Organic Frameworks for Asymmetric Heterogeneous Catalysis. *Chem. Rev.* **2012**, *112*, 1196–1231.
- (11) Zhu, Q.-L.; Li, J.; Xu, Q. Immobilizing Metal Nanoparticles to Metal-Organic Frameworks with Size and Location Control for Optimizing Catalytic Performance. *J. Am. Chem. Soc.* **2013**, *135*, 10210–10213.
- (12) Meek, S. T.; Greathouse, J. A.; Allendorf, M. D. Metal-Organic Frameworks: a Rapidly Growing Class of Versatile Nanoporous Materials. *Adv. Mater.* **2011**, *23*, 249–267.
- (13) Zhang, J.-P.; Zhang, Y.-B.; Lin, J.-B.; Chen, X.-M. Metal Azolate Frameworks: From Crystal Engineering to Functional Materials. *Chem. Rev.* **2012**, *112*, 1001–1033.
- (14) Das, M. C.; Xiang, S.; Zhang, Z.; Chen, B. Functional Mixed Metal-Organic Frameworks with Metalloligands. *Angew. Chem., Int. Ed.* **2011**, *50*, 10510–10520.
- (15) Shelnutt, J. A.; Song, X.-Z.; Ma, J.-G.; Jia, S.-L.; Jentzen, W.; Medforth, C. J. Nonplanar porphyrins and their significance in proteins. *Chem. Soc. Rev.* **1998**, *27*, 31–41.
- (16) Mansuy, D. Activation of alkanes: the biomimetic approach. *Coord. Chem. Rev.* **1993**, *125*, 129–141.
- (17) Liu, Z.; Yasserli, A. A.; Lindsey, J. S.; Bocian, D. F. Molecular Memories that Survive Silicon Device Processing and Real-World Operation. *Science* **2003**, *302*, 1543–1545.
- (18) Jiang, J.; Kasuga, K.; Arnold, D. P. In *Supramolecular Photosensitive and Electroactive Materials*; Nalwa, H. S., Eds.; Academic Press: San Diego, 2001; pp 113–210.
- (19) Suslick, K. S.; Bhyrappa, P.; Chou, J. H.; Kosal, M. E.; Nakagaki, S.; Smithenry, D. W.; Wilson, S. R. Microporous Porphyrin Solids. *Acc. Chem. Res.* **2005**, *38*, 283–291.
- (20) Scandola, F.; Chiorboli, C.; Prodi, A.; Iengo, E.; Alessio, E. Photophysical properties of metal-mediated assemblies of porphyrins. *Coord. Chem. Rev.* **2006**, *250*, 1471–1496.
- (21) Goldberg, I. Crystal engineering of porphyrin framework solids. *Chem. Commun.* **2005**, 1243–1254.
- (22) Zou, C.; Wu, C.-D. Functional porphyrinic metal-organic frameworks: crystal engineering and applications. *Dalton Trans.* **2012**, *41*, 3879–3888.
- (23) Garibay, S. J.; Stork, J. R.; Cohen, S. M. The Use of Metalloligands in Metal-Organic Frameworks. *Prog. Inorg. Chem.* **2009**, *56*, 335–378.
- (24) Zou, C.; Xie, M.-H.; Kong, G.-Q.; Wu, C.-D. Five porphyrin-core-dependent metal-organic frameworks and framework-dependent fluorescent properties. *CrystEngComm* **2012**, *14*, 4850–4856.
- (25) Xie, M.-H.; Yang, X.-L.; He, Y.; Zhang, J.; Chen, B.; Wu, C.-D. Highly Efficient C-H Oxidative Activation by a Porous Mn(III)-Porphyrin Metal-Organic Framework under Mild Conditions. *Chem.—Eur. J.* **2013**, *19*, 14316–14321.
- (26) Dolbecq, A.; Dumas, E.; Mayer, C. R.; Mialane, P. Hybrid Organic-Inorganic Polyoxometalate Compounds: From Structural Diversity to Applications. *Chem. Rev.* **2010**, *110*, 6009–6048.
- (27) Zou, C.; Zhang, Z.; Xu, X.; Gong, Q.; Li, J.; Wu, C.-D. A Multifunctional Organic-Inorganic Hybrid Structure Based on Mn^{III}-Porphyrin and Polyoxometalate as a Highly Effective Dye Scavenger and Heterogeneous Catalyst. *J. Am. Chem. Soc.* **2012**, *134*, 87–90.
- (28) Wang, X.-S.; Meng, L.; Cheng, Q.; Kim, C.; Wojtas, L.; Chrzanowski, M.; Chen, Y.-S.; Zhang, X.-P.; Ma, S. Three-Dimensional Porous Metal-Metalloporphyrin Framework Consisting of Nanoscopic Polyhedral Cages. *J. Am. Chem. Soc.* **2011**, *133*, 16322–16325.
- (29) Jin, S.; Son, H.-J.; Farha, O. K.; Wiederrecht, G. P.; Hupp, J. T. Energy Transfer from Quantum Dots to Metal-Organic Frameworks for Enhanced Light Harvesting. *J. Am. Chem. Soc.* **2013**, *135*, 955–958.
- (30) Kosal, M. E.; Chou, J.-H.; Wilson, S. R.; Suslick, K. S. A Functional Zeolite Analogue Assembled from Metalloporphyrins. *Nat. Mater.* **2002**, *1*, 118–121.
- (31) Makiura, R.; Motoyama, S.; Umeyama, Y.; Yamanaka, H.; Sakata, O.; Kitagawa, H. Surface Nano-architecture of a Metal-Organic Framework. *Nat. Mater.* **2010**, *9*, 565–571.
- (32) Lee, C. Y.; Farha, O. K.; Hong, B. J.; Sarjeant, A. A.; Nguyen, S. T.; Hupp, J. T. Light-Harvesting Metal-Organic Frameworks (MOFs): Efficient Strut-to-Strut Energy Transfer in Bipyridyl and Porphyrin-Based MOFs. *J. Am. Chem. Soc.* **2011**, *133*, 15858–15861.
- (33) Feng, D.; Gu, Z.-Y.; Li, J.-R.; Jiang, H.-L.; Wei, Z.; Zhou, H.-C. Zirconium-Metalloporphyrin PCN-222: Mesoporous Metal-Organic Frameworks with Ultrahigh Stability as Biomimetic Catalysts. *Angew. Chem., Int. Ed.* **2012**, *51*, 10307–10310.
- (34) Farha, O. K.; Shultz, A. M.; Sarjeant, A. A.; Nguyen, S. T.; Hupp, J. T. Active-Site-Accessible, Porphyrinic Metal-Organic Framework Materials. *J. Am. Chem. Soc.* **2011**, *133*, 5652–5655.

(35) Alkordi, M. H.; Liu, Y.; Larsen, R. W.; Eubank, J. F.; Eddaoudi, M. Zeolite-like Metal-Organic Frameworks as Platforms for Applications: On Metalloporphyrin-Based Catalysts. *J. Am. Chem. Soc.* **2008**, *130*, 12639–12641.

(36) Zhang, Z.; Zhang, L.; Wojtas, L.; Eddaoudi, M.; Zaworotko, M. J. Template-Directed Synthesis of Nets Based upon Octahemioctahedral Cages That Encapsulate Catalytically Active Metalloporphyrins. *J. Am. Chem. Soc.* **2012**, *134*, 928–933.

(37) Shultz, A. M.; Farha, O. K.; Hupp, J. T.; Nguyen, S. T. A Catalytically Active, Permanently Microporous MOF with Metalloporphyrin Struts. *J. Am. Chem. Soc.* **2009**, *131*, 4204–4205.

(38) Zou, C.; Zhang, T.; Xie, M.-H.; Yan, L.; Kong, G.-Q.; Yang, X.-L.; Ma, A.; Wu, C.-D. Four Metalloporphyrinic Frameworks as Heterogeneous Catalysts for Selective Oxidation and Aldol Reaction. *Inorg. Chem.* **2013**, *52*, 3620–3626.

(39) Xie, M.-H.; Yang, X.-L.; Wu, C.-D. A Metalloporphyrin functionalized metal-organic framework for selective oxidization of styrene. *Chem. Commun.* **2011**, *47*, 5521–5523.

(40) Takagi, S.; Eguchi, M.; Tryk, D. A.; Inoue, H. Porphyrin Photochemistry in Inorganic/Organic Hybrid Materials: Clays, Layered Semiconductors, Nanotubes, and Mesoporous Materials. *J. Photochem. Photobiol., C* **2006**, *7*, 104.

(41) Xie, M.-H.; Yang, X.-L.; Zou, C.; Wu, C.-D. A Sn^{IV}-Porphyrin-Based Metal-Organic Framework for the Selective Photo-Oxygenation of Phenol and Sulfides. *Inorg. Chem.* **2011**, *50*, 5318–5320.

(42) Yang, X.-L.; Xie, M.-H.; Zou, C.; He, Y.; Chen, B.; O’Keeffe, M.; Wu, C.-D. Porous Metalloporphyrinic Frameworks Constructed from Metal 5,10,15,20-Tetrakis(3,5-bis(carboxylphenyl)porphyrin for Highly Efficient and Selective Catalytic Oxidation of Alkylbenzenes. *J. Am. Chem. Soc.* **2012**, *134*, 10638–10645.

(43) Yang, X.-L.; Zou, C.; He, Y.; Zhao, M.; Chen, B.; Xiang, S.; O’Keeffe, M.; Wu, C.-D. A Stable Microporous Mixed-Metal-Organic Framework with Highly Active Cu²⁺ Sites for Efficient Cross-Dehydrogenative Coupling Reaction. *Chem. Eur. J* **2014**, *20*, 1447–1452.